Achieving High-Quality Al/Steel Joint with Ultrastrong Interface

YONGXIAN HUANG, LONG WAN, XIAOQING SI, TIFANG HUANG, XIANGCHEN MENG, and YUMING XIE

An enlarged pin head with circumferential notches for friction stir lap welding was proposed to achieve Al/steel joint with ultrastrong interface. The hook defect was eliminated. The effective interfacial width of 7.5 mm was achieved. The local silicon enrichment suppressed the growth of intermetallic compounds, which was attributed to the formation of an ultrathin interfacial layer containing a Fe_4Al_{13} layer, a single Fe_2Al_5 layer, a bright Fe-rich layer, and a chaotic layer. The maximum tensile shear strength reached up to 442 N/mm.

https://doi.org/10.1007/s11661-018-5006-4

I. INTRODUCTION

THE application of Al/steel hybrid structures in automotive industry promotes the increasing demand of lap welding techniques.[1] Fusion welding is difficult to realize the high-quality Al/steel joint due to crack, porosity, and intermetallic compounds (IMCs).[2] Friction stir lap welding (FSLW) is characterized by low peak temperature and severe plastic deformation,[3–5] which makes it a promising technique to fabricate the Al/steel joint. Many approaches have been developed to achieve excellent Al/steel FSLW joints from the viewpoints of improving mechanical interlocking and controlling the IMCs. Friction stir extrusion was proposed through extruding plasticized Al materials into a preset concave groove into steel.[6] Huang *et al.*[7] proposed self-riveting FSLW by forcing plasticized Al materials into a prefabricated hole and then producing self-riveting structure with metallurgical bonding. Wang *et al.*[8] developed friction stir scribe to realize the Al/steel lap welding and found that welding parameters highly affected microstructural features. Xiong *et al.*[9] designed a cutting pin to achieve a sound Al/steel lap joint by forming thin IMCs layer and mechanical interlocking. van der Rest *et al.*[10] developed a pinless tool to realize the Al/steel lap welding by applying frictional heat between the shoulder and the materials. Zhang *et al.*[11] proposed friction stir brazing to restrain metallurgical reaction instead of mechanically severe mixing based on a pinless tool. However, the pinless tool was always limited to the thin sheets lower than 2 mm.[12] The core of the FSLW of Al/steel is the control of the IMCs. The thinner the IMCs layer, the higher the tensile shear properties. Das *et al.*[13] and Bozzi *et al.*[14] stated that when the thicknesses of the IMCs were, respectively, 6.5 and 8 μm, the tensile shear properties were significantly improved.

An enlarged pin head with circumferential notches was developed to broaden joining interface and control the IMCs, thereby achieving an ultrastrong interface. The general defects, interfacial joining width and metallurgical bonding interface, were analyzed.

II. EXPERIMENTAL PROCEDURE

Three-millimeter-thick 6082-T6 Al and 2-mm-thick QSTE340TM steel sheets were used, the dimensions of which were all 300 × 100 mm^2. The novel FSLW tool fabricated of WC-Co alloy steel was designed as illustrated in Figure 1(a). The enlarged pin head with circumferential notches was beneficial to accelerating flow behavior of the softening materials, which further increased the effective interfacial width and avoided interfacial defects of lap joint. The diameters of the concave shoulder and the tapered right-threaded pin in bottom and top were, respectively, 14, 8, and 5 mm. The length of the novel pin was 2.85 mm. A conventional tool consisting of a shoulder of 14 mm in diameter, a cylinder pin of 6 mm in diameter, and 2.9 mm in length was applied as comparison. A rotating velocity of 1000 rpm, a welding speed of 100 mm/min, and a tilting angle of 1.5 deg with respect to *Z*-axis were used. A plunge depth of the stir pin top into the steel sheet was 0.1 mm. Schematic diagram of FSLW is displayed in Figure 1(b).

YONGXIAN HUANG, LONG WAN, XIAOQING SI, TIFANG HUANG, XIANGCHEN MENG, and YUMING XIE are with the State Key Laboratory of Advanced Welding and Joining, Harbin Institute of Technology, Harbin, 150001, P.R. China. Contact e-mail: yxhuang@hit.edu.cn
Manuscript submitted June 25, 2018.
Article published online November 8, 2018

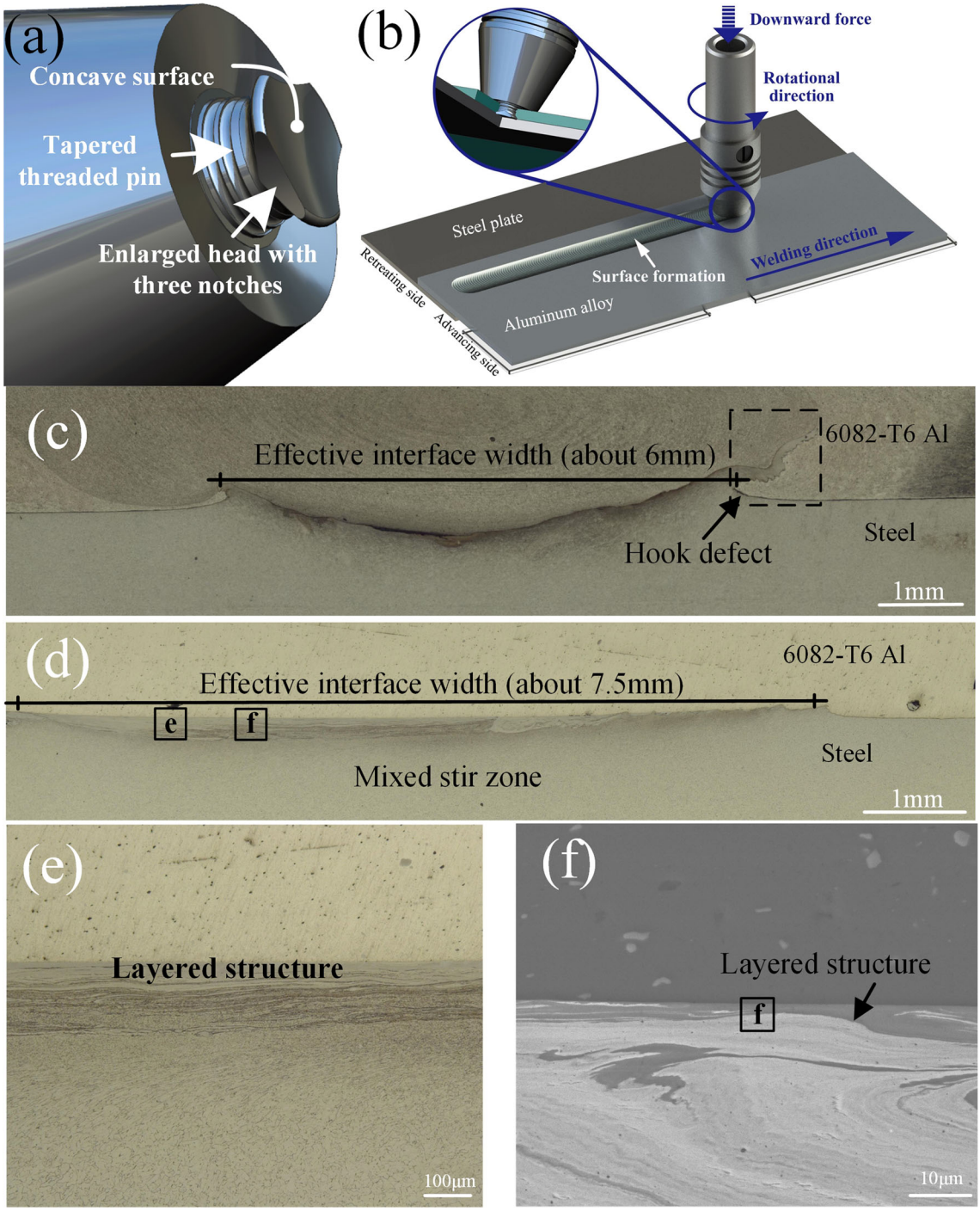

Fig. 1—Schematics: (*a*) an enlarged pin head with circumferential notches and (*b*) FSLW; macrostructures: (*c*) conventional pin and (*d*) enlarged pin head with circumferential notches; interfacial layer: (*e*) and (*f*) e and f marked in (*d*).

Specimens were cut by electrical discharge machining perpendicular to welding direction to reveal microstructures and mechanical properties. The macro and microstructures were characterized using an optical microscopy (OM), a scanning election microscopy (SEM) and a transmission electron microscope (TEM). The tensile shear tests were performed at a crosshead speed of 0.5 mm/min.

III. RESULTS AND DISCUSSION

Figure 1(c) shows the macrostructure of conventional Al/steel joint, where a hook defect appears at weld nugget zone (WNZ) of advancing side (AS). For a conventional screwed pin, the tool rotation causes the plasticized materials to flow downward along the pin screw, while the plasticized materials move far away

from the pin flow upward, resulting in the up-bending phenomenon of lap intersection and then forming the hook defect. Due to the enlarged pin head with the circumferential notches, the hook defect and chaotic layered structure disappear (Figure 1(d)). The concave design on the pin top is beneficial to improving the centripetal flow of the plasticized materials and accumulating the plasticized materials at the pin top. This phenomenon thus avoids the upward flow of the materials at the lower sheet, eliminating the hook defect. Thereby, the effective interfacial width increases from about 6.0 mm by the conventional pin to that of 7.5 mm caused by the enlarged pin head with circumferential notches (Figures 1c and d).

Figures 1(e) and (f) exhibit the interfacial layer and the IMCs layer. Detailed TEM investigations of the interfacial structure are displayed Figure 2, which consist of an outermost Fe_4Al_{13} layer with local silicon enrichment (Figures 2(a) through (c)); an adjacent single Fe_2Al_5 layer (B in Figure 2(c)), a bright Fe-rich layer, and a thin chaotic mixed layer. The local silicon enrichment layer with an average thickness of about 300 nm forms along the interface, which indicates that the interfacial structure can provide preferentially fast diffusion path for the Si atom.

Figure 2(d) exhibits a nano Fe/Al IMCs crystals less than 1.0 μm into the Al layer. Due to severe shear force and Fe outward diffusion, fine steel fragments in mixed layer dissolve in the Al and then lead to the nucleation of nano Fe_4Al_{13} crystals (Figure 2(e)). The growth direction is perpendicular to the interface at Al side. Fe_4Al_{13} crystals continuously consume the Al matrix with the increasing growth in the size and fraction. Evidently, the Fe_4Al_{13} phase preferentially grows, revealing the outward diffusion of Fe. A thin, continuous, and irregular layer of Fe_2Al_5 nucleates at the interface with abundant Fe-fragment. Concave boundaries of Fe grains in Figure 2(d) imply that Fe_2Al_5 crystals grow and react with the remaining Fe in mixed zone. Although Gibbs free energy of Fe_4Al_{13} is lower than that of Fe_2Al_5, the kinetics of reaction at Fe/Al interface result in the formation of the Fe_2Al_5 as the main constituent.[15] Phases identified in Figures 2(d) and (e) are consistent with Fe and Al concentration profiles shown in Figure 2(c). In other words, Fe atom accumulates across the interface, which represents the Fe-rich fragment—Fe_2Al_5 and Fe_4Al_{13} region—with the local silicon enrichment, and indicates the outward diffusion of Fe. Due to the three notches, there are at least three velocity fluctuations in one rotation cycle, which provides a dynamic flow,[16] and transports the plasticized Al from WNZ and the deformed Fe from the steel side. Severe shear force applied by the tool causes extreme Al grain refinement near the interface. As a result, more Al grain boundaries are available to facilitate Fe diffusion to low-Fe areas and act as nucleation sites for Fe_4Al_{13} nanocrystals (Figure 2(f)). The formation of local silicon enrichment can inhibit the

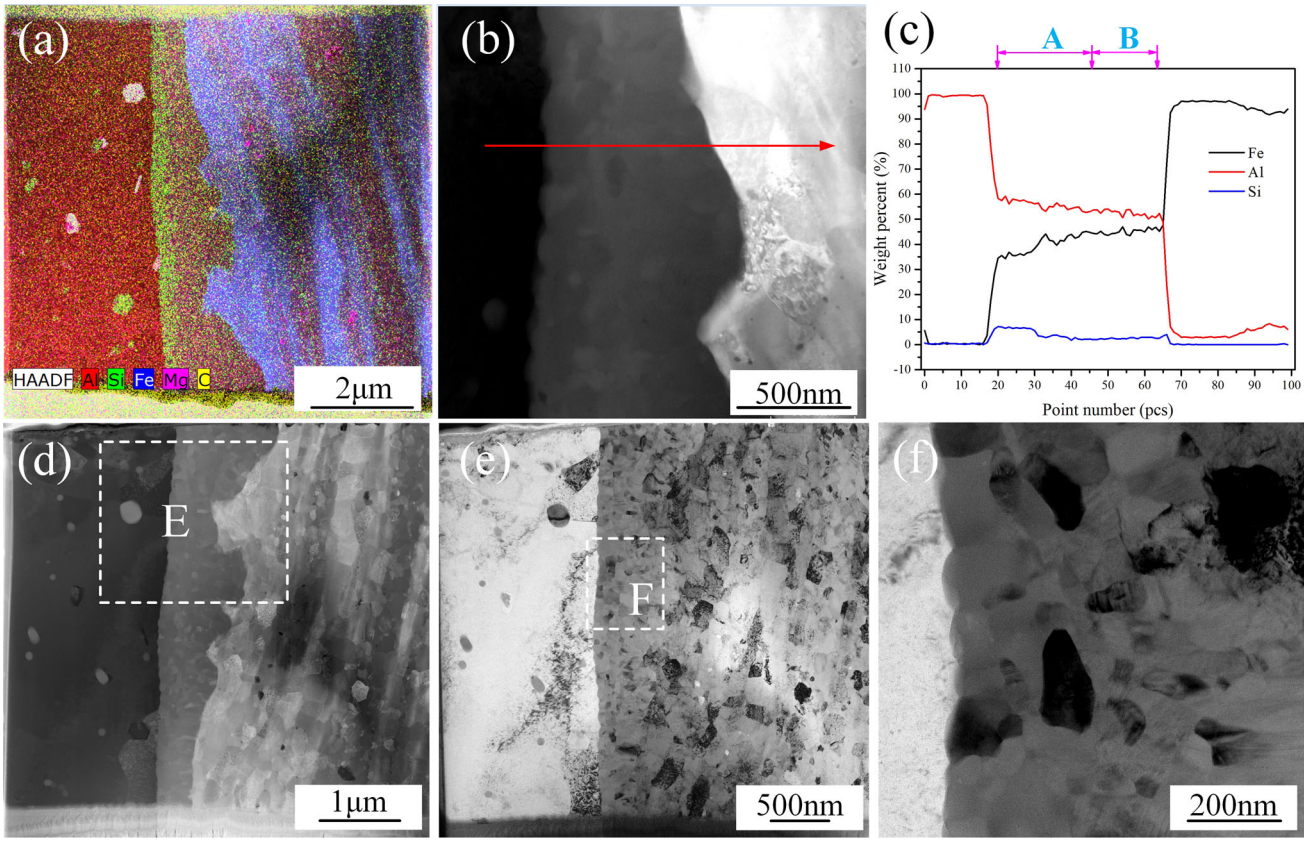

Fig. 2—STEM results of the Al/steel interface. (*a*) STEM map illustrating a locally enriched silicon layer, (*b*) layer consisting of refined intermetallic phases, (*c*) line scanning result, (*d*, *e*) morphological distributions of Fe/Al IMCs, and (*f*) enlarged view marked by "F" in (e).

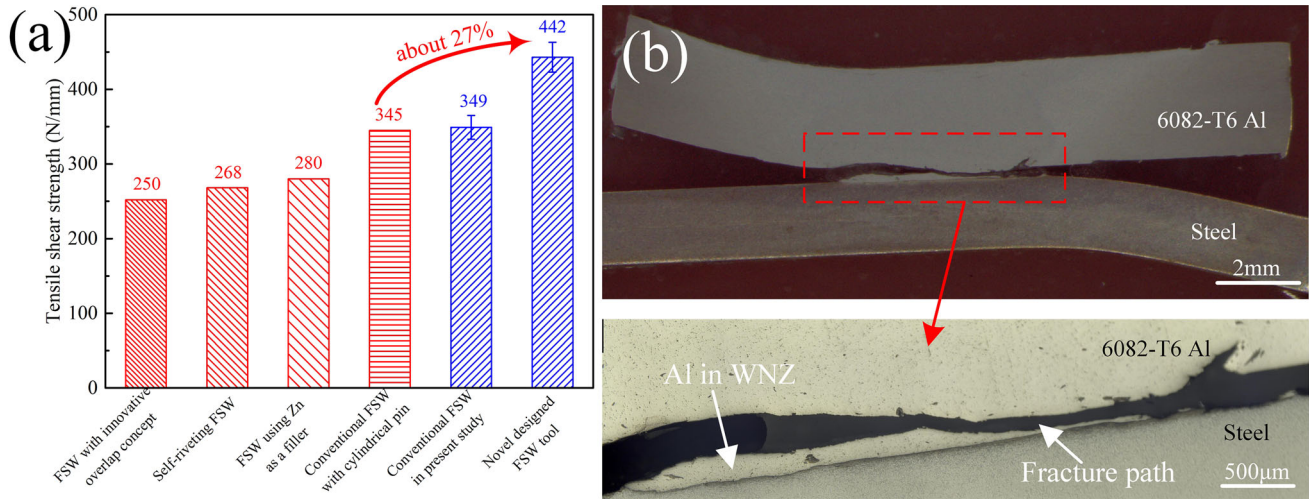

Fig. 3—(*a*) Comparisons of tensile shear strengths between four different FSW methods and the novel FSLW method, and (*b*) fracture path of Al/steel joint.

growth of the IMCs. Silicon-containing filler materials significantly limit the interdiffusion and reaction between Al and Fe, resulting in the inhibition of the IMCs during the early growth stage.[17] Therefore, an ultrastrong interface can be achieved by the metallurgical bonding with the suppressed IMCs.

To reveal the effect of the new tool on tensile shear properties, different welding methods including self-riveting FSLW,[7] FSLW with innovative overlap concept,[18] FSLW using Zn as filler metal,[19] and conventional FSLW by a cylindrical pin[20] were compared. The tensile shear strength of the Al/steel joint by the enlarged pin head with circumferential notches reaches 442 N/mm (Figure 3(a)), which is far higher than the maximum tensile shear strength of 345 N/mm reported in the published references. The improvement of tensile shear strength is attributed to the ultrastrong interfacial joint and the elimination of hook defect. Figure 3(b) shows the fracture path of the Al/steel joint by the circumferential notches of the shape pin. The fracture occurs at the WNZ of the Al side rather than at the joining interface, which indicates that interfacial joining strength is stronger than that of WNZ at the 6082-T6 alloy side. The formation of ultrastrong interface with the suppressed Fe_4Al_{13} and Fe_2Al_5 layers lower than 1 μm is beneficial to improving the interfacial joining strength. Combined with the large effective interfacial width, the ultrastrong interface as well as the elimination of the hook, the joint fracture locates at the WNZ.

IV. CONCLUSIONS

An enlarged pin head with circumferential notches was developed to achieve a high-quality Al/steel FSLW joint. The hook defect formed in the conventional joint was completely eliminated due to the centripetal flow induced by the concave shape of the pin top. The effective interfacial width of 7.5 mm was attained due to the dynamic flow caused by the three notches at the pin top, which was 2.5 times higher than the thickness of base 6082-T6 Al alloy. Significantly, an ultrathin interfacial layer could be achieved since the local silicon enrichment suppressed the further growth of the FeAl IMCs. The synthesis effects contributed to forming the ultrastrong interface. The maximum tensile shear strength reached 442 N/mm that was higher than those obtained by the other techniques. The fracture occurred at the WNZ of 6082-T6 alloy side rather than the IMCs, confirming the establishment of ultrastrong interfacial joining strength.

ACKNOWLEDGMENT

This study was supported by the National Natural Science Foundation of China (No. 51575132).

REFERENCES

1. Y.C. Chen and K. Nakata: *Metall. Mater. Trans. A*, 2008, vol. 39A, pp. 1985–92.
2. W.B. Lee, M. Schmuecker, U.A. Mercardo, G. Biallas, and S.B. Jung: *Scr. Mater.*, 2006, vol. 55, pp. 355–58.
3. H.J. Liu, H. Fujii, M. Maeda, and K. Nogi: *J. Mater. Process. Technol.*, 2003, vol. 142, pp. 692–96.
4. Y. Chen, H. Liu, and J. Feng: *Mater. Sci. Eng. A*, 2006, vol. 420, pp. 21–25.
5. T. Wang, S. Shukla, S.S. Nene, M. Frank, R.W. Wheeler, and R.S. Mishra: *Metall. Mater. Trans. A*, 2018, vol. 49A, pp. 1–5.
6. W.T. Evans, B.T. Gibson, J.T. Reynolds, A.M. Strauss, and G.E. Cook: *Manuf. Lett.*, 2015, vol. 5, pp. 25–28.
7. Y. Huang, J. Wang, L. Wan, X. Meng, H. Liu, and H. Li: *Mater. Lett.*, 2016, vol. 185, pp. 181–84.
8. T. Wang, H. Sidhar, R.S. Mishra, Y. Hovanski, P. Upadhyay, and B. Carlson: *Sci. Technol. Weld. Join.*, 2018, vol. 23, pp. 249–55.
9. J.T. Xiong, J.L. Li, J.W. Qian, F.S. Zhang, and W.D. Huang: *Sci. Technol. Weld. Join.*, 2012, vol. 17, pp. 196–201.
10. C. Van Der Rest, P.J. Jacques, and A. Simar: *Scr. Mater.*, 2014, vol. 77, pp. 25–28.

11. G. Zhang, W. Su, J. Zhang, and Z. Wei: *Metall. Mater. Trans. A*, 2011, vol. 42A, pp. 2850–61.
12. Y. Huang, X. Meng, Y. Xie, L. Wan, Z. Lv, J. Cao, and J. Feng: *Compos. A Appl. Sci. Manuf.*, 2018, vol. 105, p. 235.
13. H. Das, S.S. Jana, T.K. Pal, and A. De: *Sci. Technol. Weld. Join.*, 2014, vol. 19, pp. 69–75.
14. S. Bozzi, A.L. Helbert-Etter, T. Baudin, B. Criqui, and J.G. Kerbiguet: *Mater. Sci. Eng. A*, 2010, vol. 527, pp. 4505–09.
15. H.R. Shahverdi, M.R. Ghomashchi, and S. Shabestari: *J. Hejazi*, 2002, vol. 124, pp. 345–52.
16. Y. Huang, X. Meng, Y. Zhang, J. Cao, and J. Feng: *J. Mater. Process. Tech.*, 2017, vol. 250, pp. 313–19.
17. L. Agudo Jácome, S. Weber, A. Leitner, E. Arenholz, J. Bruckner, H. Hackl, and A.R. Pyzalla: *Adv. Eng. Mater.*, 2009, vol. 11, pp. 350–58.
18. G. Sorger, H. Wang, P. Vilaça, and T.G. Santos: *Weld. World*, 2017, vol. 61, pp. 257–68.
19. Q. Zheng, X. Feng, Y. Shen, G. Huang, and P. Zhao: *J. Alloys Compd.*, 2016, vol. 686, pp. 693–701.
20. R.S. Coelho, A. Kostka, S. Sheikhi, J.F. Dos Santos, and A.R. Pyzalla: *Adv. Eng. Mater.*, 2008, vol. 10, pp. 961–72.